Environmental Science Nano

ROYAL SOCIETY OF CHEMISTRY

PAPER

View Article Online
View Journal | View Issue



Cite this: *Environ. Sci.: Nano*, 2026, **13**, 2541

# Extraction, quantification and characterization of mercury and selenium containing nanoparticles in seal livers using single particle inductively coupled plasma time of flight mass spectrometry (spICP-ToF-MS)

Houssame-Eddine Ahabchane, [a] Chrystelle Lessard, [a] Maria Chrifi Alaoui, [b] Sofia Paciello, [b] Dominic E. Ponton, [b] Marc Amyot [b] and Kevin J. Wilkinson *[a]

Mercury accumulation in Arctic marine mammals presents significant environmental and health concerns, particularly for Indigenous communities relying on these animals as traditional food sources. This study developed a protocol for quantifying and characterizing mercury selenide (HgSe) nanoparticles in seal livers using single particle inductively coupled plasma time-of-flight mass spectrometry (spICP-ToF-MS). The initial key challenge was the extraction of the nanoparticles from the biological tissue, using the least perturbing means and simplest extraction matrix in order to preserve the HgSe nanoparticles. Five extraction methods (formic acid, proteinase & lipase, lipase, tetramethylammonium hydroxide, and ultrapure water) were compared by extracting HgSe nanoparticles from the liver of a bearded seal (*Erignathus barbatus*). Metals and metalloids in individual nanoparticles were measured by spICP-ToF-MS. Based on the particle number and the particle size distributions, formic acid was the best medium for the extraction of the HgSe nanoparticles. The HgSe nanoparticles remained structurally stable in formic acid extracts for extended periods (up to one month), with minimal changes in the particle numbers or particle size distributions. spICP-ToF-MS allowed determination of the stoichiometry of the individual HgSe nanoparticles and also revealed previously unreported trace amounts of silver (1%) and bismuth (0.5%) associated with the nanoparticles. These results expand our understanding of selenium's protective role beyond mercury sequestration, suggesting a conserved detoxification mechanism involving multi-element selenide complexes. This study establishes a robust analytical methodology for investigating metal detoxification at the nanoscale, providing insights into mercury cycling in Arctic ecosystems and exposure risks for communities consuming marine mammals.

Received 16th December 2025,
Accepted 13th April 2026

DOI: 10.1039/d5en01173f

rsc.li/es-nano



## Environmental significance

Mercury contamination in Arctic marine mammals poses direct health risks to Indigenous communities, some of which rely on these animals as traditional food sources. This study uses single particle ICP-ToF-MS to characterize mercury selenide nanoparticles from the liver of a bearded seal, providing nanoscale insight into selenium mediated mercury detoxification. The multi-elemental capability of single particle inductively coupled plasma time-of-flight mass spectrometry revealed that some of the HgSe nanoparticles also contained trace amounts of silver and bismuth, suggesting a broader detoxification mechanism involving multi-element selenide complexes. These findings advance our understanding of how biogenically produced nanomaterials can mediate mercury sequestration in biota, with implications for assessing mercury bioavailability and dietary exposure risks in Arctic ecosystems.

## Introduction

Based on the latest global assessment of natural archive records,[1] inputs of atmospheric mercury (Hg) to the Arctic have increased 5- to 9-fold compared to preindustrial times, leading to increased concern with respect to its potential effects on biota.[2] Indeed, several recent studies, in a variety

[a] *Biophysical Environmental Chemistry, Université de Montréal, 1375 Thérèse-Lavoie-Roux Ave., Montréal, QC, H2V 0B3 Canada.*
*E-mail: kj.wilkinson@umontreal.ca*
[b] *Department of Biological Sciences, Université de Montréal, 1375 Thérèse-Lavoie-Roux Ave., Montréal, QC, H2V 0B3 Canada*

of habitats, have determined high Hg levels in seabirds and marine mammals (seals, belugas, whales), particularly in the northern hemisphere.[3,4] These high concentrations have been attributed to their position at the top of the trophic level and to the significant role of biomagnification.[4] In particular, seals, which can be an important food for First Nations People, have been shown to have high Hg concentrations.[4] Among the Inuit, seal livers represent a culturally significant food source that are often consumed raw, shortly after hunting.

Methylmercury (MeHg) is particularly toxic and can accumulate in the tissues of biota, leading to serious health effects.[5] However, selenium (Se) is known to play a crucial role in mitigating the toxicity of MeHg through demethylation.[6] Indeed, there is strong evidence demonstrating direct interactions between metallothioneins and selenoproteins in which Se, in the form of selenocysteine, is used to generate mercury selenide (HgSe) micro- and nanoparticles (NPs).[7,8] Quantifying and characterizing these HgSe NPs are therefore essential for understanding the fate and potential toxicity of mercury in marine and freshwater systems.

Previous analytical approaches for HgSe NP characterization have included transmission electron microscopy (TEM),[9] laser ablation ICP-MS (LA-ICP-MS) and elemental mapping using X-ray fluorescence (XRF),[8] each of which has its limitations. For example, TEM requires extensive sample preparation and must be conducted under high vacuum, which can potentially alter the nanoparticles *via* dehydration or structural modification.[10] LA-ICP-MS requires careful and difficult calibration and standardization, with the smallest spot sizes being on the order of 1 μm. Furthermore, variations in ablation efficiency and atomic ionization can affect the consistency of the results.[11] Single particle inductively coupled plasma mass spectrometry (spICP-MS) is a relatively recent technique that allows determination of the inorganic content of nm-μm sized particles.[12] It can directly analyze individual NPs in their native state, with high sensitivity and without extensive sample preparation. Furthermore, by rapidly measuring large particle numbers, it can provide statistically useful particle concentration data and particle size distributions.[13] In a recent study, HgSe nanoparticles were extracted from seabirds and analyzed using a quadrupole-based spICP-MS. However, a limitation of the quadrupole-based technique spICP-MS is that it analyzes only a single element at a time, meaning that determinations of elemental associations are only correlative.[14] The use of a time-of-flight (ToF) device on the ICP-MS additionally allows for the determination of multiple elements in a single particle[15] (*i.e.* single particle inductively coupled plasma time-of-flight mass spectrometry or spICP-ToF-MS).

A significant challenge in the development of single particle techniques to analyze NPs in biological tissues is that it is first necessary to develop extraction methods that efficiently extract the nanoparticles, while preserving their integrity. Indeed, the extraction must be strong enough to dissolve biological tissue and maximize particle yield, while avoiding particle dissolution or agglomeration. Furthermore, the extraction medium should be simple enough to minimize matrix effects during the analysis by mass spectrometry. Various extraction methods have been documented for nanoparticles in biological tissue, including those based on enzymes,[16,17] tetramethylammonium hydroxide (TMAH)[18,19] or formic acid,[14] although these approaches have shown variable efficiencies and abilities to preserve nanoparticles from different tissue types.

The aim of this study was to first validate a protocol to efficiently extract mercury selenide (HgSe) nanoparticles from biological tissue, in this case, seal livers (*Erignathus barbatus*), for use with spICP-MS techniques. Extraction methods were verified for their ability to maximize the yield of HgSe NPs, while preserving NP integrity. Particles were then characterized by spICP-ToF-MS, allowing us to distinguish between Hg and HgSe nanodeposits, giving some insight into their potential biological availability.

## Materials and methods

### Liver samples

While several individuals and a second seal species (*Pusa hispida*) were analyzed during preliminary experiments (Table S1), liver samples from a single individual only are presented here in order to minimize the inter-sample variability and enable robust validation of the method performance. Analysis was focused on a male bearded seal (*Erignathus barbatus*) of unknown age that was hunted near the Marralik River close to Kangiqsualujjuaq in the Ungava Bay area (Fig. S1). This specimen had the highest abundance of Hg-containing nanoparticles, among all of the tested samples. The liver was cut into small pieces and freeze dried for 3 days. Lyophilized samples were then ground into powder using a glass mortar and pestle, and the final products were stored in a freezer at −20 °C until use.

### Total digestion of the liver samples

Samples were digested using a concentrated acid mixture consisting of ultra-pure nitric acid (67–70%; Plasma Pure Plus, AnalytiChem) and hydrochloric acid (34–37%; Plasma Pure, AnalytiChem) in volumes of 4 mL and 1 mL, respectively. Microwave-assisted digestion was performed using a MARS 5 microwave system following the U.S. Environmental Protection Agency (EPA) Method 3051.[20] Mercury Hg and Se concentrations were quantified in diluted digests using a NexION 5000 triple quadrupole ICP-MS (PerkinElmer Inc., Massachusetts, USA). Instrumental operating conditions are summarized in Table S2. External calibration curves for Hg and Se (1, 2, 5, 10, and 20 μg $L^{-1}$) were prepared from single-element standards (AnalytiChem, Montréal, Canada) obtained from 1000 mg $L^{-1}$ stock solutions. Internal standards consisted of yttrium for selenium and bismuth for mercury (10 μg $L^{-1}$; AnalytiChem,

 

Montréal, Canada). A separate quality control standard (AnalytiChem, Montréal, Canada) was analyzed to validate the ICP-MS measurements, and analytical accuracy was verified using the certified reference material DOLT-5 (dogfish liver).[21] The isotopes $^{202}$Hg and $^{82}$Se were monitored in normal mode.

### Extraction methods

For the extraction methods described below, we aimed to find the best possible approach that would be the least perturbing for the NPs. Protocols were taken from previously published extraction protocols,[8,14,16–18,22–25] though only the El Hanafi *et al.* paper[14] previously analyzed HgSe particles, albeit by SP ICP-MS. For each of the protocols, 5 mL of an extraction solution was added to 20 mg of powdered, freeze-dried seal liver in a 15 mL conical polypropylene tube.

(i) Lipase:[16,18] at least 5250 units of lipase from *Candida rugosa* (Sigma-Aldrich, USA, 1.5 mg mL$^{-1}$) were added to 0.025% (v/v) Triton-X-100 (Sigma-Aldrich, USA) in 5 mL of 5 mM HEPES (4-(2-hydroxyethyl)-1-piperazineethanesulfonic acid) (Fisher Scientific, Montréal, Canada) adjusted to pH ~7.5 using NaOH.

(ii) Proteinase & lipase:[17] the powdered sample was first mixed with 5 mL of diethyl ether in a 15 mL tube. The mixture was shaken at 150 rpm for 1 hour on a rotary shaker, and then centrifuged. The ether phase containing the lipids was transferred to a new tube, taking care to remove the lipids completely. Twenty mg of proteinase from *Aspergillus melleus* type XXIII (Sigma-Aldrich, USA, ≥3 units mg$^{-1}$ solid) and 10 mg of lipase from *Candida rugosa* type VII (Sigma-Aldrich, USA) were added to 5 mL of 50 mM ammonium bicarbonate (pH adjusted to 7.4 with HCl). Finally, 12.5 μL of Triton-X-100 was added to the mixture to give a concentration of 0.025% (v/v).

(iii) Tetramethylammonium hydroxide (TMAH) solution:[18,19] the powdered seal liver was added to 5 mL of 10% TMAH (v/v) (Alfa Aesar, Massachusetts, USA) containing 0.025% (v/v) Triton-X-100.

(iv) Formic acid solution:[14,18] five mL of a 50% HCOOH (v/v) solution (J.T. Baker, USA) was mixed with the seal liver; 0.025% (v/v) Triton-X-100 was added to the mixture.

(v) Milli-Q water: five mL of Milli-Q water containing 0.025% (v/v) Triton-X-100 was used both as a control and as an extremely simplified matrix.

For all five extraction protocols, mixtures were initially vortexed for 30 seconds to ensure a homogeneous suspension. They were then sonicated for 15 minutes at 25% amplitude in an ice bath using pulse mode (50 seconds on, 10 seconds off; QSONICA500 ultrasonicator, New Town, USA; 500 watts). Following sonication, samples were centrifuged at 1000 × *g* for five minutes to remove larger particles and undigested tissue fragments. Supernatants were carefully collected and diluted 100× for use with spICP-ToF-MS analysis. Procedural blanks were processed identically to the samples, in order to monitor contamination of the different steps of the protocol.

### Validation using commercial HgSe particles

To the best of our knowledge, reference materials containing Hg and Se in known ratios are not available for purchase. Therefore, in order to validate Se : Hg molar ratios that were obtained from the different extraction methods, a sample of bulk HgSe (PURATREM, USA) was suspended in ultrapure water in the presence of 0.05% Triton X-100. The surfactant was essential since without it, the nanoparticles strongly adhered to the tube's walls. Samples were then centrifuged (1000 × *g*, 5 minutes) in order to remove larger agglomerates. The particles in the resulting supernatant were characterized for their hydrodynamic diameters by dynamic light scattering (DLS, Wyatt Technology), following validation using 60 nm polystyrene nanospheres (Bangs Laboratories) (measured 64.0 ± 0.5 nm, %PDI 3.3 ± 1.7%). The resulting well dispersed HgSe particles were then used as a reference system for measurements of the particle molar ratios in the different extraction media.

### spICP-ToF-MS

Nanoparticles were analyzed using a time-of-flight ICP-MS (Vitesse, Nu Instruments, Wrexham, UK) run in high speed (single particle) mode. The instrument sensitivity for $^{197}$Au (used to convert signal intensity to analyte mass) was determined using a series of ionic standards purchased from AnalytiChem (Canada) and prepared in 2% v/v $HNO_3$ for Au (1, 2, 5, 10, and 20 μg L$^{-1}$). Two ultra-uniform gold nanoparticle suspensions (50 nm and 100 nm; NanoComposix, San Diego, CA, USA) were used to determine transport efficiency. Measurements were validated by analyzing the particle size distribution of a uniform suspension of silver nanoparticles (60 nm; NanoComposix, San Diego, CA, USA). Multi-elemental standard curves were prepared from a commercial standard (IV-ICPMS-71A; Inorganic Ventures, Christianburg, VA, USA) with added Bi and Hg (AnalytiChem; Canada) at 1, 2, 5, 10, and 20 μg L$^{-1}$ in 2% v/v $HNO_3$ + 0.5% v/v HCl. To ensure maximum accuracy and stability, all Hg standards were freshly prepared from a 1000 mg L$^{-1}$ stock solution on the same day as the analysis.

Prior to spICP-ToF-MS analysis, all samples and calibration solutions were vortexed for 30 seconds, and then placed in an ultrasonic bath (5510R-DTH Bransonic®, DANBURY USA) for ten minutes in order to disperse agglomerated particles. Depending on the concentration, multiple dilutions were performed (50× to 1000×) by diluting samples in ultrapure water. Elemental compositions of the samples were determined over the mass range 60–210 amu. Three replicates were analyzed for each sample. Data were collected over 60 seconds using two dwell times (80 and 190 μsec). The complete operating conditions for the spICP-ToF-MS are provided in Table S2.

### Data analysis

Raw data were processed using *IsotopeTrack*[26] application that implemented the SPCal algorithm, which assumed a

compound Poisson lognormal ion distribution.[27] CSV files containing information on the ion counts, masses and moles of each element in each particle, were processed using a custom script that was prepared in Python 3.11.5 using the Streamlit app *TOFVision*.[28] Particle concentrations were determined from eqn (1):

$$C = \frac{P \times f}{\eta \times t} \quad (1)$$

where $C$ represents the concentration of particles $mL^{-1}$, $P$ is the particle count or the number of peaks observed in the time scan, $\eta$ is the calibrated transport rate ($\mu L\ s^{-1}$), $t$ is the total acquisition time ($s$) and $f$ is the dilution factor. Particle mass distributions were determined directly by the spICP-ToF-MS based on the ionic calibrations. A one-way ANOVA followed by Tukey's HSD *post-hoc* test was used for statistical comparisons between the extraction methods.

## Results and discussion

### Optimization of the extraction conditions

Total mercury and selenium concentrations were first determined in the livers of several seal species using quantitative ICP-MS following complete acid digestion (Table S3). Of the different samples examined, the bearded seal liver contained exceptionally high concentrations of both mercury (425.9 ± 5.1 μg $g^{-1}$ dry weight) and selenium (172.6 ± 2.5 μg $g^{-1}$ dry weight) with a molar ratio of Se : Hg of 1.03, making it an ideal candidate for further investigation. In addition, MeHg concentrations were determined and found to be quite low (2.015 μg $g^{-1}$ dry weight) (SI Text S1).

During method development, sample mass, ultrasonication conditions (time, amplitude, mode), temperature and post-treatment methods were tested in order to identify the method that gave the greatest number of particles (Table S4) as determined from the number of spICP-ToF-MS peaks. Indeed, the time-resolved signals revealed distinct peaks for both mercury and selenium, with frequent co-localization of the elements within individual particle events (Fig. 1).

Particle numbers were considered to be the most important criteria for optimization of the extraction, as they reflect not only the efficiency of the extraction, but also the detection limits for spICP-ToF-MS analysis. Indeed, in spICP-ToF-MS, reduced background will normally result in greater numbers of particles being detected[29] since dissolved forms of the metal(loid)s can mask the particulate forms of the metals, especially for the smallest nanoparticles. Comparison of the extraction protocols revealed significant differences in the extraction efficiencies. The formic acid protocol yielded the highest number of mercury-containing particles ((5.5 ± 0.1) × $10^6$ particles $mL^{-1}$), followed by the lipase-based protocol ((6.5 ± 0.2) × $10^5$ particles $mL^{-1}$), ultrapure water ((5.3 ± 0.1) × $10^5$ particles $mL^{-1}$), TMAH ((4.6 ± 0.8) × $10^5$ particles $mL^{-1}$), and finally proteinase & lipase ((2.2 ± 0.1) × $10^5$ particles $mL^{-1}$) (Table S5). This was a strong indication that the formic acid protocol was the best of the five, though the lipase protocol was also observed to have performed well.

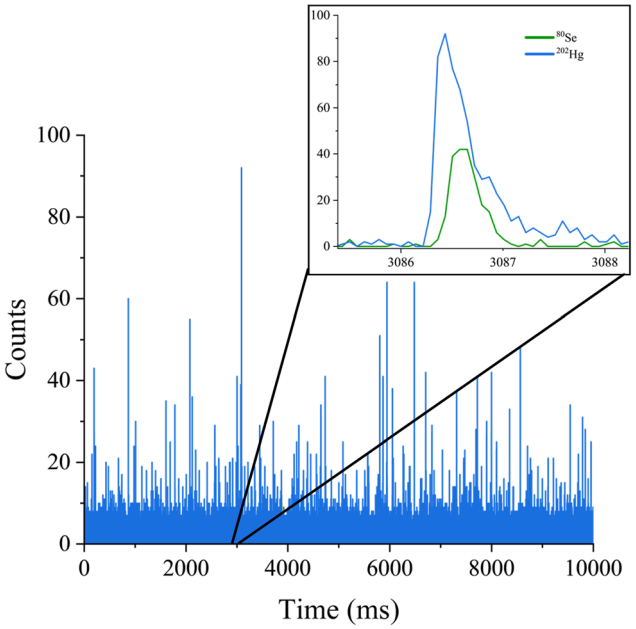


Fig. 1 Ten seconds of the transient signal obtained by spICP-ToF-MS following the extraction of the bearded seal livers using formic acid. Inset: Expanded scale (3085–3088 ms) is for a single peak where both selenium (green) and mercury (blue) can be observed in a single ion cloud (*i.e.* single nanoparticle).

### Recovery of selenium and mercury by spICP-ToF-MS relative to total acid digestion and analysis by ICP-MS

The sum of particulate and dissolved concentrations determined by spICP-ToF-MS were compared to Se and Hg concentrations obtained by quantitative acid digestion for each extraction protocol (Table 1). The concentrations of Se and Hg in the nanodeposits were also compared with the acid digested samples in order to quantify their importance.

With respect to the recoveries of Se and Hg, the formic acid and TMAH protocols performed best for both elements, with recoveries near 100% for Se (formic acid: 99.7 ± 5.2%; TMAH: 110.1 ± 8.2%) and ~80% for Hg (formic acid: 76.0 ± 6.9%; TMAH: 85.7 ± 3.7%). While the selenium recovery by TMAH slightly exceeded 100%, this is reasonable given the high efficiency of the TMAH extraction for dissolving biological matter[18] (even with respect to acid digestion). However, while TMAH gave high recoveries for Hg and Se, very few particles were detected, suggesting that they were dissolved by the more aggressive alkaline chemistry of the treatment. In addition, there is some analytical uncertainty inherent to all spICP-MS techniques, as samples are generally not acidified during analysis and adsorptive losses are possible.

**Table 1** Mean ± SD for the recovery of selenium and mercury by spICP-ToF-MS relative to total acid digestion for each extraction protocol. Values are calculated from 3 biological replicates, each analyzed in triplicate. Total recovery includes both particulate Hg and Se and contributions from the dissolved background. The fraction of Se and Hg that was in the form of nanodeposits was also calculated by dividing the nanoparticle signal by the values obtained by total acid digestion

| Extraction method | Se recovery (%) | Hg recovery (%) | Fraction of Se in particulate form (%) | Fraction of Hg in particulate form (%) |
|---|---|---|---|---|
| HCOOH | 99.7 ± 5.2 | 76.0 ± 6.9 | 6.4 ± 0.4 | 7.8 ± 0.7 |
| TMAH | 110.1 ± 8.2 | 85.7 ± 3.7 | 1.9 ± 0.2 | 1.0 ± 0.0 |
| Lipase | 7.9 ± 1.2 | 4.1 ± 0.2 | $(5.0 \pm 1.2) \times 10^{-4}$ | $(6.0 \pm 1.5) \times 10^{-4}$ |
| Proteinase + lipase | 7.0 ± 4.0 | 1.7 ± 0.6 | $(2.4 \pm 0.7) \times 10^{-4}$ | $(3.4 \pm 1.0) \times 10^{-4}$ |
| Ultrapure water | 5.7 ± 0.6 | 5.0 ± 0.3 | $(5.2 \pm 1.5) \times 10^{-4}$ | $(5.4 \pm 1.0) \times 10^{-4}$ |

Even though the formic acid extraction yielded the highest particle numbers ($(5.5 \pm 0.1) \times 10^6$ particles $mL^{-1}$, Table S5), the proportion of Hg and Se that were detected as nanoparticles remained low (Se: 6.4 ± 0.4%; Hg: 7.8 ± 0.7%). Admittedly, without the ability to spike the samples with a reference material, the presence of particles is not sufficient evidence to indicate that the extraction was performed under optimal conditions. For example, the extraction conditions could hypothetically allow for an artifactual precipitation of dissolved Hg and Se into nanoparticulate forms, leading to an overestimation. Nonetheless, when ionic Hg and Se were mixed in formic acid and processed through the same analytical workflow, no nanoparticle events were detected, supporting the interpretation that the particles detected in the formic acid extraction media were largely native to the tissue. On the other hand, underestimations of HgSe particles are also possible, given that a non-negligible fraction of particles, particularly the smallest ones, will inevitably fall below the size detection limits of the instrument (SDL: Se 110.2 nm, Hg 79.1 nm for formic acid; Table S5). This implies that particles with sizes that were below the SDL will contribute to the bulk element signal but will not be counted as discrete particle events. Indeed, even with marginally lower SDLs for the enzymatic and water-based protocols (Se ~100 nm and Hg ~67–70 nm), few particles were detected ($2.2–6.5 \times 10^5$ particles $mL^{-1}$ *vs.* $5.5 \times 10^6$ particles $mL^{-1}$ for formic acid), consistent with the incomplete degradation of the tissue matrix. Indeed, for the water, lipase and proteinase/lipase extractions, only 5.7–7.0% of the total Se and 1.7–5.0% of the total Hg were recovered, indicating that these gentler protocols were unable to liberate the majority of the tissue-bound Hg and Se. In other words, a marginally better SDL is of limited benefit when the extraction itself fails to release particles in sufficient numbers from the biological tissue.

### Validation of the protocols based on measured particle masses, particle contents and molar ratios

Given the dual role of the media on the extraction efficiency and the instrumental detection limits, the use of particle masses and particle contents is necessarily more nuanced for optimizing the particle extractions. In this case, particle masses and particle contents were compared with the assumed least aggressive extraction, *i.e.* ultrapure water. Our hypothesis was that, with respect to the extraction in water, particle mass gains would indicate an agglomeration, while particle mass losses would be indicative of dissolution. Similarly, changes to the proportions of Hg : HgSe NP with respect to what was observed in water or variations in the Se : Hg ratios would be indicative of selective perturbations of the Hg species.

Significant differences were observed among the particle mass distributions obtained using the different extraction methods (one-way ANOVA, Tukey's HSD *post-hoc* testing, $\alpha = 0.05$) (Table 2). While all methods showed some differences, when compared to the particle masses in water, the mass of Hg single element particles was closest for the lipase extraction, differing by only −6.7 fg ($p = 0.375$), while the proteinase protocol showed a moderate deviation from the water protocol (−14.7 fg, $p = 0.017$). Formic acid showed a moderate increase (+20.3 fg, $p = 0.002$), while TMAH showed the largest differences with respect to water, with much larger (but far fewer) particles being observed (+72.5 fg, $p < 0.001$). On the other hand, for determinations of the HgSe particle mass, the lipase protocol (−5.8 fg, $p = 0.803$) and the proteinase protocol (−14.3 fg, $p = 0.202$) showed apparent decreases, which were not significant. Finally, formic acid showed a substantial increase compared to water (+33.1 fg, $p < 0.001$). The largest positive deviation with respect to water (+96.2 fg, $p < 0.001$) was observed when extracting the HgSe particles with TMAH. Indeed, the TMAH extraction yielded distributions with fewer but substantially larger particles, suggesting that agglomeration was occurring. Such observations are consistent with a recent study,[30] which suggested that the TMAH extraction of tissues can substantially alter particle number and particle mass distributions, resulting in significant transformations of the target nanomaterials.

Based on the particle masses, the method using proteinase would appear to induce slight particle dissolution, while the formic acid would appear to cause some particle agglomeration. Both the enzymatic and formic acid protocols appeared to be superior to the TMAH extraction. Based on the limited data on previously reported sizes of the Hg nanodeposits[14] (formic acid 215 ± 90 nm; enzymatic 148 ± 58 nm), all of the particle sizes found here (formic acid: Hg 172 ± 41 nm; lipase: Hg 121 ± 31 nm; proteinase + lipase: Hg 100

**Table 2** Differences between particle masses in the extraction media with respect to the ultrapure water control (one-way ANOVA, Tukey's HSD *post-hoc* testing, $\alpha$ = 0.05). 3 biological replicates and 3 analytical replicates were analyzed per method. For the values in bold, masses and diameters were not significantly different from water extracted values

| Method | Hg mass *vs.* water (fg) | HgSe mass *vs.* water (fg) |
|---|---|---|
| TMAH | +72.5 ($p < 0.001$) | **+96.2** ($p < 0.001$) |
| Formic acid (HCOOH) | +20.3 ($p = 0.002$) | **+33.1** ($p < 0.001$) |
| Lipase | **−6.7 ($p < 0.375$)** | **−5.8** ($p = 0.803$) |
| Proteinase + lipase | −14.7 ($p < 0.017$) | **−14.3** ($p = 0.202$) |

± 19 nm; ultrapure water: Hg 142 ± 28 nm) appear reasonable, for all of the extraction media. A final consideration: it is possible that the observed deviations resulted from the ICP-ToF-MS measurement (matrix effects, *e.g.* in ref. 31) and not from the extraction. This possibility was minimized by analyzing samples that were diluted 100× prior to their analysis by spICP-ToF-MS.

With respect to the individual particle types, the formic acid extraction recovered substantially more Hg particles (2107 *vs.* 254 in water, ~8.3-fold increase) and dramatically more HgSe particles (1707 *vs.* 112 in water, ~15.2-fold increase). In contrast, the proteinase/lipase extraction showed reduced Hg particle recovery compared to water (50 particles, 0.20-fold) and a similar extraction of HgSe particles (99 particles, 0.88-fold). The lipase protocol showed slightly enhanced extraction for both particle types (Hg: 280 particles, 1.1-fold; HgSe: 178 particles, 1.6-fold). TMAH extracted similar numbers of Hg particles compared to water (246 particles, 0.97-fold) but fewer HgSe particles (77 particles, 0.69-fold).

In order to further validate the spICP-ToF-MS technique for the determination of HgSe NPs, each extraction medium was spiked with the same volume (100 µL) of a reference suspension of HgSe in the absence of the biological tissue. The suspension was then sonicated continuously for 15 minutes, and aliquots were immediately diluted 100× and analyzed. The analyzed (diluted) samples contained between approximately 350 and 800 detected particles for a 3-minute acquisition.

One of the motivations for quantifying HgSe NPs involves the determination of the Se : Hg molar ratios within individual particles. Analysis of the reference suspensions of HgSe (Fig. 2) revealed that a Se : Hg molar ratio close to 1 : 1 (1.0 ± 0.3), as expected for stoichiometric HgSe nanoparticles, was only obtained in ultrapure water. The 1 : 1 stoichiometry was independently confirmed by the total acid digestion of the HgSe powder, followed by analysis using both ICP-ToF-MS (Nu Vitesse) and ICP-MS (NeXION 5000) (Text S3, SI). In contrast, all other extraction media showed varying degrees of selenium enrichment. TMAH and formic acid yielded

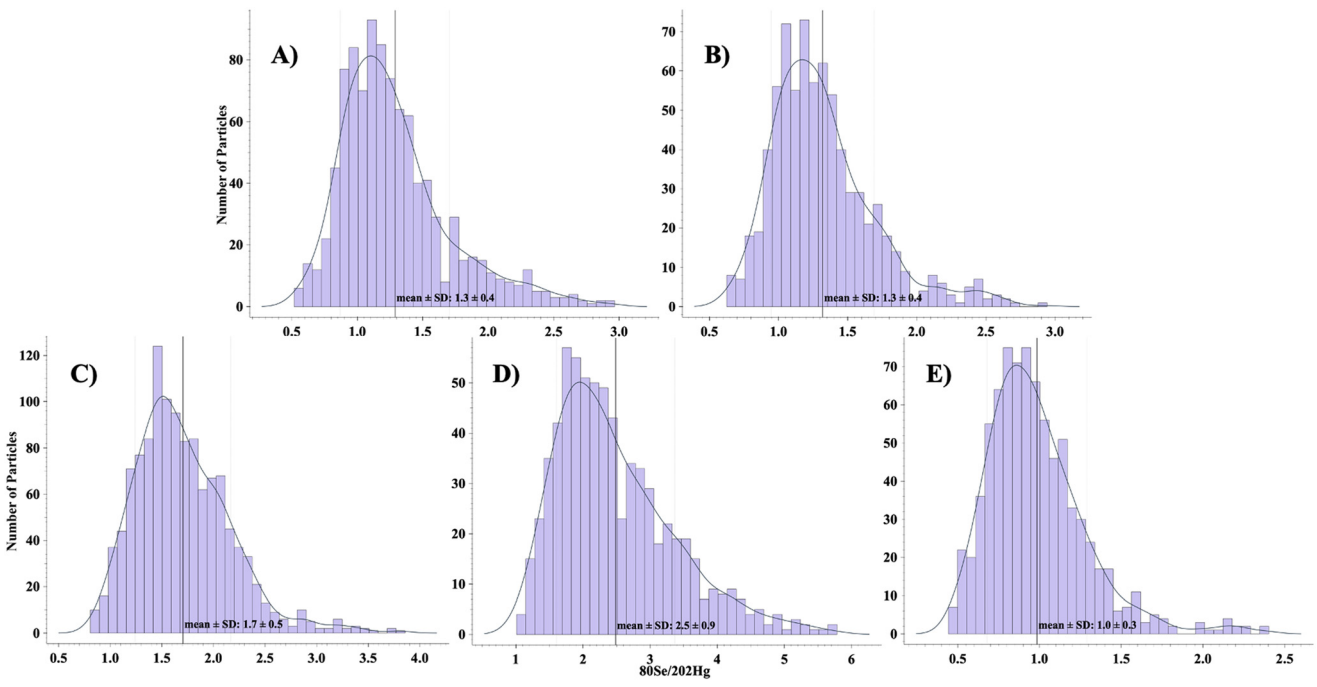


**Fig. 2** The Se : Hg molar ratio ($^{80}Se/^{202}Hg$) measured in the powder HgSe particle suspension after exposure to different extraction solutions: A) TMAH (tetramethylammonium hydroxide), B) formic acid (HCOOH), C) lipase, D) proteinase + lipase and E) ultrapure water. The mean ± SD represents three replicates and three analyses.

 

similar, slightly elevated values (1.3 ± 0.4 for both methods) while the enzymatic digestions gave statistically higher Se : Hg ratios, with the particles in lipase giving 1.7 ± 0.5 and the particles in proteinase + lipase giving values of 2.5 ± 0.9. The elevated Se : Hg ratios are an indication that in the presence of the enzymes, either selenium was preferentially re-adsorbed on the HgSe particles following their partial degradation (*i.e.* dissolution) or some Hg was being lost (*e.g.* sorptive losses to the container walls, volatilisation).

Molar ratios were also examined for extracted tissue (Fig. 3). In that case, Se : Hg molar ratios of 1.3 ± 0.5 were obtained for the water extraction, in close alignment with values of ~1.25–1.67 reported for aqueous extraction of HgSe NP from sperm whale livers.[32] The TMAH extraction produced slightly lower ratios of 1.0 ± 0.4, while formic acid extraction yielded ratios of 1.5 ± 0.6, both statistically similar to the water extraction. On the other hand, as above, both enzymatic extractions resulted in substantially higher Se : Hg ratios with proteinase/lipase yielding a ratio of 3.6 ± 1.2 and lipase giving a value of 2.1 ± 0.8. Clearly, in the presence of the enzymatic media, elevated Se : Hg ratios were observed, in the presence or absence of the biological matrix.

Based on the substantially higher particle numbers obtained for the formic acid extraction, in addition to the reasonable conservation of masses and Se : Hg molar ratios that were observed, it was concluded that the formic acid was the preferred method for the extraction of the Hg and HgSe NPs from the seal livers. Its efficiency can be attributed to its ability to denature proteins and disrupt cell membranes while maintaining a moderately acidic environment (pH 2.6 ± 0.2) that optimizes particle recovery without causing severe dissolution or agglomeration of the HgSe NPs. Note that due to its acidic nature, it is unlikely that this extraction medium would be suitable for other highly soluble NPs, such as ZnO, CuO or Ag.[33,34]

### Stability of HgSe particles in formic acid

After establishing formic acid as the best extraction method, it was necessary to determine the stability of the NPs in the formic acid extracts. Samples were extracted using formic acid, then diluted 100× and stored at 4 °C for varying durations, ranging from 1 hour to 1 month, prior to their analysis by spICP-ToF-MS. Importantly, all samples were analyzed on the same day in order to reduce analytical variability due to day-to-day instrumental variation. This experimental design allowed us to determine whether prolonged storage in formic acid (pH 2.6 ± 0.2) would affect the integrity, size distribution, or concentration of the extracted HgSe nanoparticles. Such a stability assessment is crucial for establishing proper sample handling protocols and maximum holding times of the extracted samples before analysis. Additionally, the stability of the NPs at pH 2.6, which approximates the acidity of the human gastric environment, provides preliminary insights into how these particles might behave during human digestion.

Particle mass distributions of Se and of Hg in the nanoparticles were verified over time. Elemental masses (Fig. 4) and particle numbers (Fig. 5) were stable over time, with only a few minor fluctuations, strongly indicating that

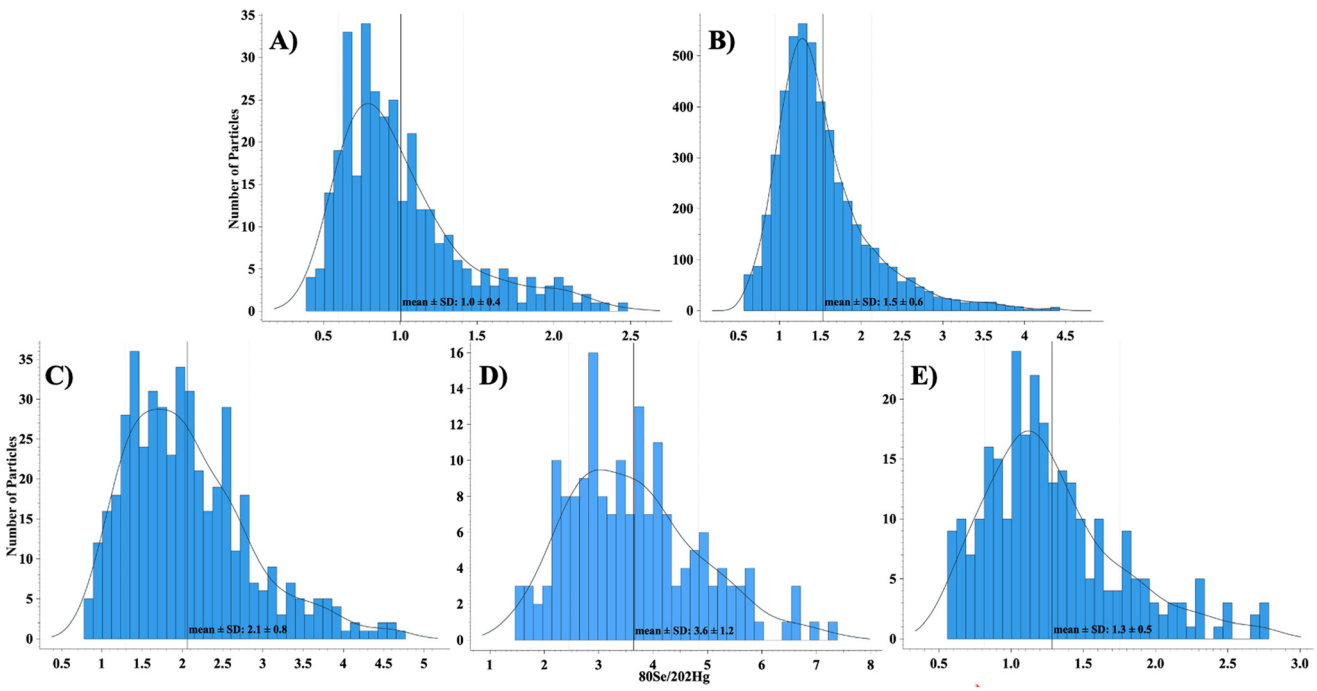


**Fig. 3** Se : Hg molar ratios for the individual nanoparticles, obtained using the different extraction methods. The vertical lines correspond to the mean from the combined data for three biological replicates, each analyzed in triplicate: (A) TMAH (tetramethylammonium hydroxide), (B) formic acid (HCOOH), (C) lipase, (D) proteinase + lipase, and (E) ultrapure water. The mean ± SD is determined from the three biological replicates.

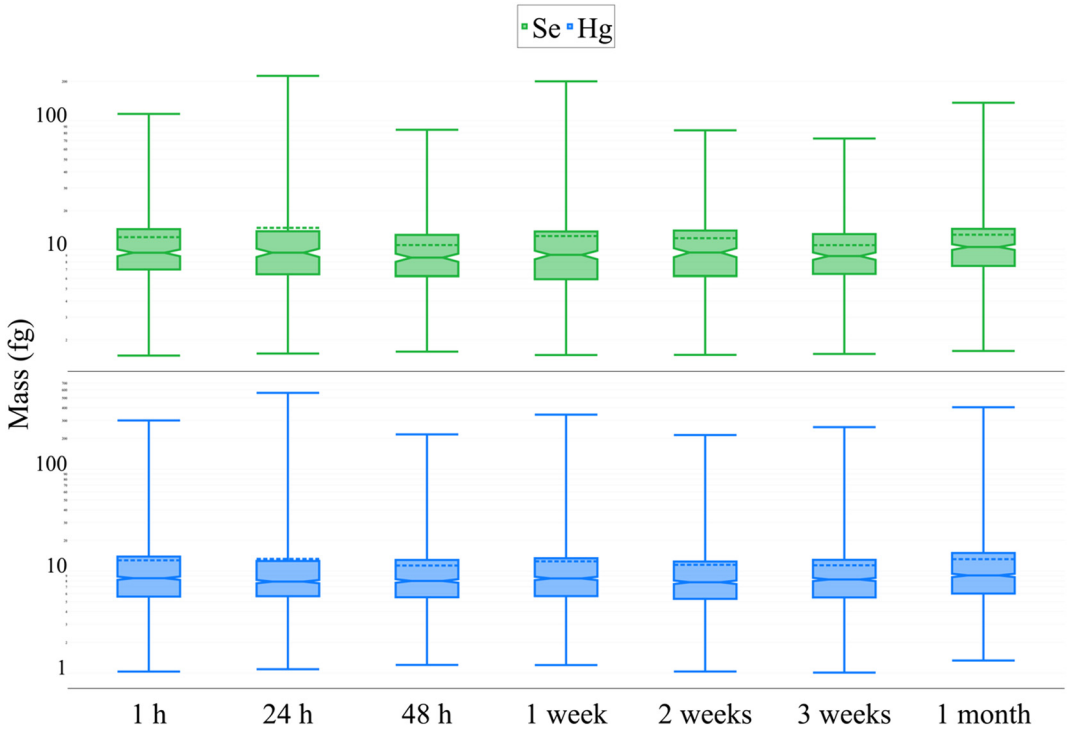


Fig. 4 Long-term stability of Hg (bottom) and Se (top) particle mass distributions in a formic acid extract for 1 hour to 1 month. Box and whisker plot was provided to summarize data. The dashed line represents the mean of the mass.

the extraction medium was non-perturbing over these relatively long-term studies. In Fig. 5, the variability of particle number measurements was ±8.2%, which is well within the typical analytical variability for nanoparticle concentration measurements (particle mass/diameter measurements generally show less analytical variability than particle numbers).

Particle mass distributions of Hg and Se nanoparticles remained stable throughout the one-month observation period (Fig. 5). The data include all particle detections (single-element Se or Hg particles and multi-element HgSe particles). After 1 h, the mean Se and Hg masses were 12.4 ± 11.2 fg and 12.7 ± 17.3 fg, respectively, while after one month they remained nearly identical at 13.0 ± 11.5 fg for Se and 13.1 ± 16.7 fg for Hg. When considering only particles containing both Se and Hg (true HgSe nanoparticles), higher masses were observed: 12.9 ± 11.2 fg for Se and 27.6 ± 30.5 fg for Hg at 1 h, and 13.4 ± 11.5 fg for Se and 26.2 ± 28.2 fg for Hg after one month. Regardless of the particle population considered, both the mean and the variability (SD) of the mass distributions remained stable. The data indicate that storage in formic acid (pH 2.6 ± 0.2) did not induce any detectable dissolution, aggregation, or compositional changes in the HgSe nanoparticles.

### Nature of the Se : Hg nanoparticles

The simultaneous detection of Hg and Se within discrete signal pulses provides strong evidence for the presence of HgSe nanoparticles in the seal liver extracts. These findings are consistent with a recent paper by Paton *et al.* (2024), who employed spICP-ToF-MS to characterize HgSe nanoparticles in whale tissue. Their study documented similar spectral signatures, strengthening the hypothesis that selenium-facilitated sequestration represents a widespread biological strategy for mitigating mercury toxicity in marine mammals.

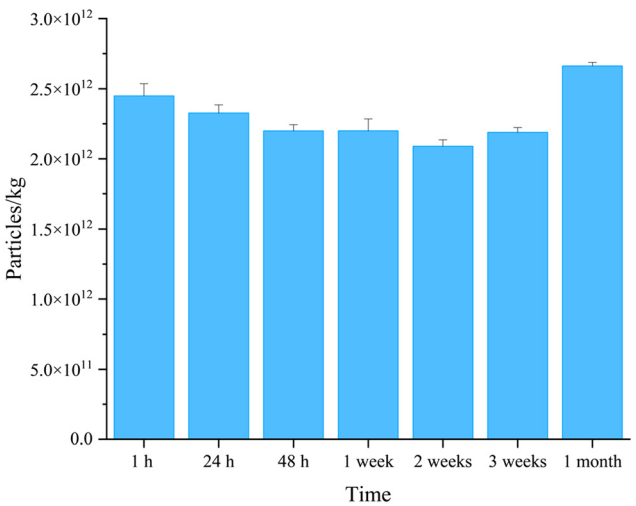


Fig. 5 Number concentrations of Hg-containing particles extracted from a bearded seal liver using formic acid extraction (pH = 2.6 ± 0.2) and kept for up to one month of storage. Data are expressed as particles $kg^{-1}$ dry weight.

 

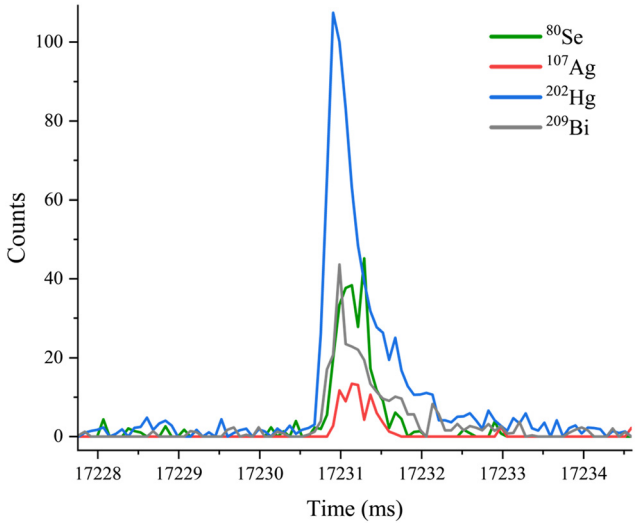


Fig. 6 Transient mass spectrometry signal for selenium (green), silver (red), mercury (blue) and bismuth (grey) containing nanoparticles observed by spICP-ToF-MS, following an extraction of the bearded seal liver using formic acid.

Interestingly, in our samples, silver and bismuth were also detected in some of the HgSe nanoparticles. For example, the transient mass spectrometry signal from Fig. 1 was re-processed, but with silver and bismuth added to the output (Fig. 6). These results show that selenium not only interacts with mercury to reduce its toxicity, but it may also be associated with other toxic elements that would normally be perceived as being harmful to the immune system. In the Paton *et al.* (2024) paper, Cd and Sn were identified as secondary elements in the particles alongside Hg and Se in the whale tissue, however, these elements were not observed in our analyses. The possibility that selenium actively detoxifies silver by forming insoluble, biologically inert selenide phases is supported by observations in marine mammals and in laboratory studies.[23] In that work, the authors demonstrated that selenium not only forms HgSe complexes for mercury detoxification, but also binds silver in the form of $Ag_2Se$ granules within hepatic tissues, highlighting a broader detoxification role.[23] Safaei *et al.* (2025) also showed that nanoparticulate selenium can attenuate the toxicity of silver nanoparticles in mice, speculating that after the initial formation of HgSe nanocrystals, selenium could continue to incorporate and immobilize other trace metals, such as silver, through secondary sequestration into the HgSe matrix.[35] A similar process could potentially occur with bismuth, given its known chemical affinity for selenium and the stability of BiSe compounds.[36] Nonetheless, these remain hypothetical pathways, representing plausible extensions of selenium-mediated detoxification, which will warrant further experimental validation. In any case, the consistent association of selenium with multiple toxic elements, across different marine mammal species (seals in our study and whales in Paton's work), suggests a conserved detoxification mechanism involving selenium sequestration.

Finally, a heatmap was generated from the data for these 4 elements. Eight particle combinations were detected: Hg, Hg–Se, Bi–Hg–Se, Se, Ag–Bi–Hg–Se, Ag–Hg–Se, Bi–Hg, and Bi, with average molar proportions shown in Fig. 7. Note that the particle numbers in parentheses were generated from 540 seconds of analysis (sample intake of 450 μL $min^{-1}$ with an average transport efficiency of 22.98 μL $min^{-1}$). When extrapolated to the entire liver, the most prevalent combination was for Hg alone ($0.7 \times 10^{12}$ particles $kg^{-1}$ dry weight) and HgSe NPs ($0.4 \times 10^{12}$ particles $kg^{-1}$). However, numerous HgSe particles ($1.6 \times 10^{11}$ particles $kg^{-1}$) were also found to contain Ag and Bi, with a low molar proportion of silver and bismuth, averaging 1.0% and 0.5% respectively, in which case, the molar proportions of selenium and mercury averaged 56.9% and 42.0%, respectively. These proportions are similar to the NPs where only Se (58.8%) and Hg (41.2%) were detected.

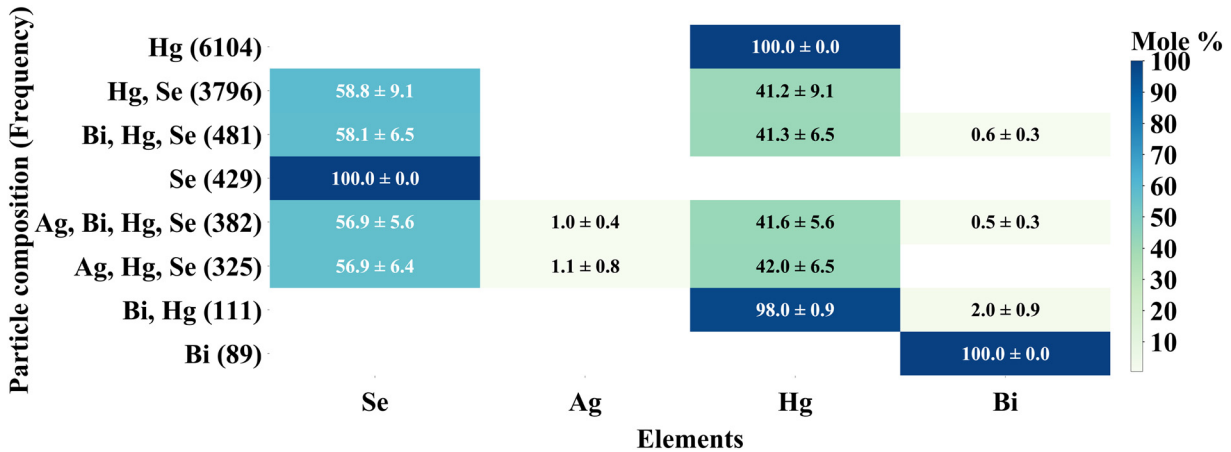


Fig. 7 Heatmap of the detected particles containing Se, Ag, Hg or Bi (or a combination thereof). Particle numbers in parentheses refer to a sample that was diluted 100× (9 minutes analysis time, transport efficiency = 0.383 μL $s^{-1}$). The annotation on the heatmap gives the average molar percent (±standard deviations) for each element in the particle. Particles were extracted from ~20 mg of a bearded seal liver using 5 mL of formic acid.

The trace amounts of silver and bismuth (~1%) in some of the HgSe nanoparticles suggested that selenium may play a broader role than previously thought in detoxifying multiple heavy metals. Silver, while less frequently studied than mercury in Arctic ecosystems, is also known to be toxic to aquatic organisms at elevated concentrations.[37,38] On the other hand, bismuth has received little scientific attention with respect to its concentrations or its potential toxicological significance in Arctic marine mammals. Its incorporation into stable selenide nanoparticles may represent a biological detoxification mechanism or may simply be fortuitous complexation.

When analysing spICP-ToF-MS results, it is always important to consider size or mass detection limits (DLs) since in some cases, the detection of a single element can simply mean that the second element was not detected (rather than not being present). Mass detection limits of selenium (0.3 fg) and mercury (0.1 fg) were reasonably similar here (Table S6), implying that for the cases where only Hg was detected, it is likely that little or no Se was actually present. Another important consideration is that lighter elements are not systematically analysed by this technique, so that Hg-containing particles could also be associated with non-quantified elements such as sulfur or carbon. The mass range was deliberately limited to 60–210 amu in order to optimize instrument sensitivity and detection capabilities for the target elements. In cases where sulfur was included by adjusting the RF voltages in the reaction cell to favor lower mass elements, reduced sensitivity was observed for the higher mass elements (Se, Ag, Hg and Bi). Nonetheless, while S-containing particles could be detected through instrumental optimization (*e.g.*, a particle containing S, Se, Ag, Hg, and Bi; Fig. S3 in the SI), such multi-element particles were rare in the analyzed samples.

Numerous studies have reported correlations between total mercury and other elements (particularly selenium, but also silver and other metals) in marine mammal tissues,[39] however, they were limited to bulk chemical analyses that couldn't confirm the physical associations of the elements. Our direct observation of multi-element nanoparticles strengthens the mechanistic explanation for these widely reported elemental correlations, demonstrating that the co-occurrence of these elements in marine mammal tissues is likely to be in the form of complex nanoparticulate structures rather than fortuitous associations. The multi-element binding capacity of selenium likely represents an important adaptive mechanism that allows marine mammals to tolerate exposure to mercury, but perhaps also to other chalcophile elements, such as Ag and Bi, which also have a high affinity for selenium.[32] The formation of these complex, multi-element selenide particles may be an effective strategy for simultaneously reducing the bioavailability of several potentially harmful elements.

## Conclusion

This work establishes an analytical framework for elucidating complex metal detoxification processes at the nanoscale. The methodologies used here will enable more comprehensive monitoring of Arctic environmental health while providing valuable information for assessing dietary mercury exposure risks in communities that depend on marine mammals as a traditional food source. Formic acid was established as the best protocol for isolating HgSe NPs from seal liver tissue where little evidence was observed for modifications to the particles. Stability studies demonstrated that HgSe NPs maintained their structural integrity in the formic acid extracts for extended periods (up to one month), with minimal changes in particle number or particle mass distributions. While this protocol appeared to be best suited for extracting the HgSe NPs from the studied tissue, the lipase extraction can be a useful alternative, despite somewhat lower recoveries. It might be useful for other NP types.

The use of spICP-ToF-MS allowed for novel insights into the complex nature of these multi-element nanoparticles, with some containing not just mercury and selenium, but also silver. This finding expands our understanding of selenium's protective role in marine mammals beyond mercury sequestration and gives us better insight into the detoxification mechanism. Finally, future research is required in at least three key directions: (1) comparative analysis of these multi-element selenide nanoparticles across different tissues and marine mammal species; (2) investigation of the stability and bioavailability of these particles during human digestion; and (3) exploration of the molecular and cellular mechanisms governing the formation of these complex nanoparticles.

## Author contributions

Houssame-Eddine Ahabchane wrote the initial drafts of the paper, developed and conducted the experiments, treated and acquired much of the data, and arranged them into figures and tables. Chrystelle Lessard conducted some of the preliminary experiments, designed Table S4 and the graphical abstract, and contributed to the drafts of the paper. Maria Chrifi Alaoui conducted some of the experiments and contributed to the drafts of the paper. Sofia Paciello assisted with the experimental work and data collection. Dominic Ponton provided valuable practical suggestions and guidance throughout the study. Marc Amyot and Kevin Wilkinson provided resources for the experiments, contributed to the conceptualization, offered practical suggestions, and contributed to data interpretation and to the writing of all drafts of the paper.

## Conflicts of interest

There are no conflicts to declare.

 

## Data availability

Much of the data supporting this article are included as part of the supplementary information (SI). Raw data are shared at https://doi.org/10.5281/zenodo.19731329.

Supplementary information: containing information on the examined seals, the sampling location, ICP-ToF-MS/ICP-MS operating conditions, CRM recoveries, MeHg analyses, tested extraction protocols, measured HgSe particle numbers, measured HgSe molar ratios, HgSe particle size distributions, LOD, LOQ, MDL, MQL, SDL, SQL values for the formic acid extraction, transient mass spectrometry signal showing multiple elements. See DOI: https://doi.org/10.1039/d5en01173f.

## Acknowledgements

We acknowledge the financial support of the NSERC Alliance grants, the NSERC Discovery grant program and the Canada Research Chair program. We extend our sincere gratitude to the Inuit community for their collaboration and for providing the liver samples that were essential to this research. Special thanks are given to Madjid Hadioui, Dominic Belanger and Aaron J. Goodman for their technical assistance and support. We also acknowledge the mechanical engineering workshops at the University of Montreal campus MIL for their contribution to this work.

## References

1 Q. Chen, Q. Wu, Y. Cui and S. Wang, Mercury records from natural archives reveal ecosystem responses to changing atmospheric deposition, *Natl. Sci. Rev.*, 2024, **11**(12), nwae417, DOI: 10.1093/nsr/nwae417, (acccessed 6/16/2025).

2 AMAP, 2018. AMAP Assessment 2018: Biological Effects of Contaminants on Arctic Wildlife and Fish. *Arctic Monitoring and Assessment Programme (AMAP)*, Tromsø, Norway, vii +84pp, "https://www.amap.no/documents/doc/amap-assessment-2018-biological-effects-of-contaminants-on-arctic-wildlife-and-fish/1663"; "https://www.amap.no/documents/doc/amap-assessment-2018-biological-effects-of-contaminants-on-arctic-wildlife-and-fish/1663.

3 R. Dietz, P. M. Outridge and K. A. Hobson, Anthropogenic contributions to mercury levels in present-day Arctic animals —A review, *Sci. Total Environ.*, 2009, **407**(24), 6120–6131, DOI: 10.1016/j.scitotenv.2009.08.036.

4 D. J. Yurkowski, E. McCulloch, W. R. Ogloff, K. F. Johnson, R. Amiraux, N. Basu, K. H. Elliott, A. T. Fisk, S. H. Ferguson and L. N. Harris, *et al.*, Mercury accumulation, biomagnification, and relationships to δ13C, δ15N and δ34S of fishes and marine mammals in a coastal Arctic marine food web, *Mar. Pollut. Bull.*, 2023, **193**, 115233, DOI: 10.1016/j.marpolbul.2023.115233.

5 M. Houde, Z. E. Taranu, X. Wang, B. Young, P. Gagnon, S. H. Ferguson, M. Kwan and D. C. G. Muir, Mercury in Ringed Seals (Pusa hispida) from the Canadian Arctic in Relation to Time and Climate Parameters, *Environ. Toxicol. Chem.*, 2020, **39**(12), 2462–2474, DOI: 10.1002/etc.4865.

6 M. J. Berry and N. V. Ralston, Mercury toxicity and the mitigating role of selenium, *Ecohealth*, 2008, **5**(4), 456–459, DOI: 10.1007/s10393-008-0204-y, From NLM.

7 G. Barone, A. Storelli, D. Meleleo, A. Dambrosio, R. Garofalo and A. Busco, Storelli, M. M. Levels of Mercury, Methylmercury and Selenium in Fish: Insights into Children Food Safety, *Toxics*, 2021, **9**(2), 39–52; W. B. Minich, Selenium Metabolism and Biosynthesis of Selenoproteins in the Human Body, *Biochemistry*, 2022, **87**(1), S168–S177, DOI: 10.1134/S0006297922140139.

8 Z. Gajdosechova, M. M. Lawan, D. S. Urgast, A. Raab, K. G. Scheckel, E. Lombi, P. M. Kopittke, K. Loeschner, E. H. Larsen and G. Woods, *et al.*, In vivo formation of natural HgSe nanoparticles in the liver and brain of pilot whales, *Sci. Rep.*, 2016, **6**(1), 34361, DOI: 10.1038/srep34361.

9 X. Ji, L. Yang, F. Wu, L. Yao, B. Yu, X. Liu, Y. Yin, L. Hu, G. Qu and J. Fu, *et al.*, Identification of mercury-containing nanoparticles in the liver and muscle of cetaceans, *J. Hazard. Mater.*, 2022, **424**, 127759, DOI: 10.1016/j.jhazmat.2021.127759.

10 C. Mühlfeld, B. Rothen-Rutishauser, D. Vanhecke, F. Blank, P. Gehr and M. Ochs, Visualization and quantitative analysis of nanoparticles in the respiratory tract by transmission electron microscopy, *Part. Fibre Toxicol.*, 2007, **4**(1), 11–27, DOI: 10.1186/1743-8977-4-11.

11 M. Martinez and M. Baudelet, Calibration strategies for elemental analysis of biological samples by LA-ICP-MS and LIBS – A review, *Anal. Bioanal. Chem.*, 2020, **412**(1), 27–36, DOI: 10.1007/s00216-019-02195-1.

12 C. Degueldre and P. Y. Favarger, Colloid analysis by single particle inductively coupled plasma-mass spectroscopy: a feasibility study, *Colloids Surf., A*, 2003, **217**(1), 137–142, DOI: 10.1016/S0927-7757(02)00568-X.

13 H. E. Pace, N. J. Rogers, C. Jarolimek, V. A. Coleman, C. P. Higgins and J. F. Ranville, Determining transport efficiency for the purpose of counting and sizing nanoparticles via single particle inductively coupled plasma mass spectrometry, *Anal. Chem.*, 2011, **83**(24), 9361–9369, DOI: 10.1021/ac201952t, From NLM.

14 K. El Hanafi, B. Gomez-Gomez, Z. Pedrero, P. Bustamante, Y. Cherel, D. Amouroux and Y. Madrid, Simple and rapid formic acid sample treatment for the isolation of HgSe nanoparticles from animal tissues, *Anal. Chim. Acta*, 2023, **1250**, 340952.

15 Z. Li, M. Hadioui and K. J. Wilkinson, Extraction of Silicon-Containing Nanoparticles from an Agricultural Soil for Analysis by Single Particle Sector Field and Time-of-Flight Inductively Coupled Plasma Mass Spectrometry, *Nanomaterials*, 2023, **13**(14), 2049–2060.

16 M. V. Taboada-López, P. Herbello-Hermelo, R. Domínguez-González, P. Bermejo-Barrera and A. Moreda-Piñeiro, Enzymatic hydrolysis as a sample pre-treatment for titanium dioxide nanoparticles assessment in surimi (crab sticks) by single particle ICP-MS, *Talanta*, 2019, **195**, 23–32, DOI: 10.1016/j.talanta.2018.11.023, From NLM.

17 K. Loeschner, J. Navratilova, C. Købler, K. Mølhave, S. Wagner, F. von der Kammer and E. H. Larsen, Detection and characterization of silver nanoparticles in chicken meat by

asymmetric flow field flow fractionation with detection by conventional or single particle ICP-MS, *Anal. Bioanal. Chem.*, 2013, **405**(25), 8185–8195, DOI: 10.1007/s00216-013-7228-z, From NLM.

18 A. Chalifoux, M. Hadioui, N. Amiri and K. J. Wilkinson, Analysis of Silver nanoparticles in ground beef by single particle inductively coupled plasma mass spectrometry (SP-ICP-MS), *Molecules*, 2023, **28**(11), 4442–4455.

19 J. Gruszka, J. Malejko, A. Bajguz and B. Godlewska-Żyłkiewicz, Method development for speciation analysis of silver nanoparticles and silver ions in green algae and surface waters at environmentally relevant concentrations using single particle ICP-MS, *J. Anal. At. Spectrom.*, 2022, **37**(6), 1208–1222, DOI: 10.1039/D2JA00032F.

20 C. Element, Method 3051A microwave assisted acid digestion of sediments, sludges, soils, and oils, *Anal. Bioanal. Chem.*, 2007, **111**, 362–366.

21 L. Yang, S. Willie, P. Grinberg, I. Pihillagawa Gedara, V. Clancy, P. Maxwell, G. McRae, C. Palmer, K. Kubachka and M. Wolle, *et al.*, DOLT-5: Dogfish Liver Certified Reference Material for Trace Metals and other Constituents DOLT-5 : Foie de chien de mer, matériau de référence certifié pour les métaux traces et d'autres constituants, National Research Council Canada Conseil national de recherches Canada, 2014.

22 B. L. Batista, D. Grotto, J. L. Rodrigues, V. C. Souza and F. Barbosa Jr., Determination of trace elements in biological samples by inductively coupled plasma mass spectrometry with tetramethylammonium hydroxide solubilization at room temperature, *Anal. Chim. Acta*, 2009, **646**(1–2), 23–29, DOI: 10.1016/j.aca.2009.05.022, From NLM.

23 T. Ikemoto, T. Kunito, H. Tanaka, N. Baba, N. Miyazaki and S. Tanabe, Detoxification mechanism of heavy metals in marine mammals and seabirds: interaction of selenium with mercury, silver, copper, zinc, and cadmium in liver, *Arch. Environ. Contam. Toxicol.*, 2004, **47**(3), 402–413, DOI: 10.1007/s00244-004-3188-9, From NLM.

24 A. Naganuma and N. Imura, Properties of mercury and selenium in a high-molecular weight substance in rabbit tissues formed by simultaneous administration, *Pharmacol., Biochem. Behav.*, 1981, **15**(3), 449–454, DOI: 10.1016/0091-3057(81)90276-8, From NLM.

25 G. Tao, S. N. Willie and R. E. Sturgeon, Determination of total mercury in biological tissues by flow injection cold vapour generation atomic absorption spectrometry following tetramethylammonium hydroxide digestion, *Analyst*, 1998, **123**(6), 1215–1218, DOI: 10.1039/a802000k, From NLM.

26 H. E. Ahabchane, A. J. Goodman, M. Hadioui and K. J. Wilkinson, IsotopeTrack: a fast and flexible application for the analysis of SP-ICP-TOF-MS datasets, *Environ. Chem.*, 2026, **23**(2), EN25111, DOI: 10.1071/EN25111.

27 T. E. Lockwood, L. Schlatt and D. Clases, SPCal – an open source, easy-to-use processing platform for ICP-TOFMS-based single event data, *J. Anal. At. Spectrom.*, 2025, **40**(1), 130–136, DOI: 10.1039/D4JA00241E.

28 H.-E. Ahabchane, A. Wu and K. J. Wilkinson, SP-TOF-ICP-MS Analysis 'TOFVision', https://github.com/Houssame-EA/TOFVision, 2024, https://github.com/Houssame-EA/TOFVision (accessed 2025 11 June).

29 M. Hadioui, C. Peyrot and K. J. Wilkinson, Improvements to single particle ICPMS by the online coupling of ion exchange resins, *Anal. Chem.*, 2014, **86**(10), 4668–4674, DOI: 10.1021/ac5004932, From NLM.

30 B. Sadeghalvad and E. P. Gray, Evaluation of alternative bases to TMAH for tissue extraction of ENMs from tissues prior to spICP-MS analysis, *Environ. Sci.: Nano*, 2024, **11**(10), 4309–4320, DOI: 10.1039/D4EN00416G.

31 S. Harycki and A. Gundlach-Graham, Single-Particle ICP-TOFMS with Online Microdroplet Calibration: A Versatile Approach for Accurate Quantification of Nanoparticles, Submicron Particles, and Microplastics in Seawater, *Anal. Chem.*, 2023, **95**(41), 15318–15324, DOI: 10.1021/acs.analchem.3c02785, From NLM.

32 L. Paton, T. T. Moro, T. Lockwood, T. de Andrade Maranhão, G. Gössler, D. Clases and J. Feldmann, AF4-MALS-SP ICP-ToF-MS analysis gives insight into nature of HgSe nanoparticles formed by cetaceans, *Environ. Sci.: Nano*, 2024, **11**(5), 1883–1890, DOI: 10.1039/D3EN00886J.

33 M. Hadioui, S. Leclerc and K. J. Wilkinson, Multimethod quantification of Ag+ release from nanosilver, *Talanta*, 2013, **105**, 15–19, DOI: 10.1016/j.talanta.2012.11.048.

34 L. Fréchette-Viens, M. Hadioui and K. J. Wilkinson, Quantification of ZnO nanoparticles and other Zn containing colloids in natural waters using a high sensitivity single particle ICP-MS, *Talanta*, 2019, **200**, 156–162, DOI: 10.1016/j.talanta.2019.03.041.

35 S. Safaei, M. Azarnia, E. Amini, M. Nabiuni and M. Abdollahian, Selenium nanoparticles attenuates silver nanoparticles toxicity in mice Sertoli cells via modulation of SOD and Kindlin-2, *J. Trace Elem. Med. Biol.*, 2025, **91**, 127720, DOI: 10.1016/j.jtemb.2025.127720.

36 X. Lin, H. Xie, Y. Zhang, X. Wang, Y. Ma, H. Zhang, C. Hao, S. Mu, Q. Liu and Q. Li, *et al.*, Using bismuth selenide nanoparticles to combat methylmercury-induced neurodegeneration, *Ecotoxicol. Environ. Saf.*, 2025, **303**, 119031, DOI: 10.1016/j.ecoenv.2025.119031.

37 K. Saeki, M. Nakajima, T. R. Loughlin, D. C. Calkins, N. Baba, M. Kiyota and R. Tatsukawa, Accumulation of silver in the liver of three species of pinnipeds, *Environ. Pollut.*, 2001, **112**(1), 19–25, DOI: 10.1016/S0269-7491(00)00103-2.

38 I. Delgado-Suarez, E. Lozano-Bilbao, A. Hardisson, S. Paz and Á. J. Gutiérrez, Metal and trace element concentrations in cetaceans worldwide: A review, *Mar. Pollut. Bull.*, 2023, **192**, 115010, DOI: 10.1016/j.marpolbul.2023.115010.

39 G. López-Berenguer, J. Peñalver and E. Martínez-López, A critical review about neurotoxic effects in marine mammals of mercury and other trace elements, *Chemosphere*, 2020, **246**, 125688, DOI: 10.1016/j.chemosphere.2019.125688, From NLM.

 